1-1-1992

Scaling Behavior Of The Ising-Model Coupled To 2-Dimensional Quantum-Gravity

Simon M. Catterall

John B. Kogut

Ray L. Renken
University of Central Florida

Scaling behavior of the Ising model coupled to two-dimensional quantum gravity

S. M. Catterall and J. B. Kogut
Loomis Laboratory of Physics, University of Illinois at Urbana-Champaign, 1110 West Green Street, Urbana, Illinois 61801

R. L. Renken
University of Central Florida, Orlando, Florida 32816

(Received 21 November 1991)

We study the Ising model on dynamical ϕ^3 graphs with spherical topology. A finite-size scaling analysis is carried out both with and without an external field leading to numerical estimates for various critical exponents which are in good agreement with analytical calculations. We further determine the equation of state, and measure the correlation of Ising spins on the ensemble of graphs.

PACS number(s): 11.15.Ha, 11.17.+y, 64.60.Fr

I. INTRODUCTION AND MODEL

String theory in a Euclidean space can be thought of as a theory of free bosons coupled to two-dimensional quantum gravity. While classically the dimension of the embedding space is a free parameter, the quantum theory is only tractable analytically in the critical dimension $D=26$ where the gravity sector effectively decouples. To try to analyze the structure of the subcritical theory various authors [1,2,3] have proposed the use of a regulated model based on dynamically triangulated random surfaces. It is natural to try to extend this to the case of fermionic strings, i.e., to add anticommuting degrees of freedom to the discretized world sheet. It is well known that the Ising model on an arbitrary random graph is equivalent in the critical region to a Majorana fermion [4]. We are thus motivated to consider the partition function of an Ising model coupled to (discrete) quantum gravity,

$$Z=\sum_{G_N}\sum_{\sigma_i} e^{S(J,H)} ,$$

$$S=J\sum_{\langle ij\rangle}\sigma_i\sigma_j+H\sum_i\sigma_i .$$

The numerical results we shall describe here were concerned with the application of careful finite-size scaling techniques to this model to locate the onset of a scaling regime, and to subsequently extract reliable estimates for certain critical exponents. While previous numerical approaches have utilized a triangulated lattice and worked only in the limit when $H=0$, we were able to test universality by working on the dual lattice and at nonzero field. This allowed a first measurement of the magnetic exponent δ and a determination of the equation of state. By providing extensive tables of data, we hope our results will, in addition, be of use to others working on related systems. We also attempt the first numerical or analytical determination of the correlation-length exponent governing the behavior of the two-point function on the ensemble of graphs.

We have employed a microcanonical ensemble where the number of vertices N is held fixed. By allowing two loops in a graph to have at most one link in common we have eliminated all degeneracies associated with tadpoles and self-energy insertions. We further confine ourselves to graphs with the topology of the sphere. Since our prime interest will be a numerical measurement of the critical exponents, which are independent of genus, this is not an important restriction. A simple Metropolis algorithm is used to implement changes in the Ising spins and local reconnections of the ϕ^3 graph. For details of the vector program we use to generate configurations we refer the reader to [5].

The model has been solved analytically by exploiting its equivalence to a large-N matrix model [6]. The system undergoes a third-order phase transition (in zero field H) between a low- and high-temperature (small J) phase with a set of critical exponents which differ markedly from their values on a fixed lattice. It came as a surprise, therefore, when a numerical study of this model by Gross *et al.* [7] produced only the fixed lattice exponents. However, in this case the authors used a Regge approach for simulating the gravity sector.

Since this model is one of the few which admit an exact solution, it serves as an important testing ground for our numerical techniques. Specifically, how well do our Monte Carlo simulations, which attempt to estimate the summation over graphs, produce exponents in agreement with the analytical prediction? The results of such a study allow us to tune the algorithms and give us confidence in interpreting the numerical results from other models where analytic solution is not possible.

Borrowing traditional ideas from statistical mechanics we will primarily be interested in studying the finite-size behavior of various quantities close to the infinite-lattice critical coupling $J_c=\frac{1}{2}\ln(108/23)$. A precise knowledge of J_c eliminates a huge source of error in the analysis of the finite-lattice data. One further difficulty arises in applying these standard techniques: the necessity of extracting a linear scale L for these dynamical systems. This we do by setting

$$L\sim N^{1/d} .$$

The exponent d is an intrinsic Hausdorff dimension characterizing the internal geometry of the graph. The finite-size scaling ansatz requires any thermodynamic function Q, measured on a finite lattice close to criticality, to be given by some scaling form [8]

$$Q(J,N)=N^{x/\nu d}f(\epsilon N^{1/\nu d}) .$$

The quantity $\epsilon=|1-J_c/J|$ measures the deviation away from the infinite-lattice critical point. The argument of the function f is essentially the ratio of the correlation length to the linear size of the system. The exponents x and ν are defined from the infinite-lattice singularities of Q and the correlation length ξ:

$$Q(J)\sim(J-J_c)^{-x} ,$$

$$\xi(J)\sim(J-J_c)^{-\nu} .$$

Notice that the ratio $x/\nu d$ can be measured by setting $\epsilon=0$, i.e., $J=J_c$ and analyzing the N dependence of Q

$$Q(J_c,N)\sim f(0)N^{x/\nu d} .$$

In order that we recover the infinite-lattice result $Q\sim\epsilon^{-x}$ as $N\to\infty$, the scaling function $f(z)$ must have the asymptotic behavior

$$f(z)\sim z^{-x} .$$

Thus a measurement of the limiting behavior of the scaling function also allows a determination of critical exponents. We have considered two primary observables, the magnetization M with exponent β and the susceptibility χ with corresponding exponent γ:

$$M=\frac{1}{N}\sum_i \sigma_i, \quad M\sim(J-J_c)^{\beta} ,$$

$$\chi=N(\langle M^2\rangle-\langle M\rangle^2), \quad \chi\sim(J-J_c)^{-\gamma} .$$

Using the results of the previous discussion we have attempted to derive estimates for ratios of the critical exponents $\beta/\nu d$ and $\gamma/\nu d$. To help reduce some of the tunneling effects on finite lattices for $J>J_c$ we have replaced M by $|M|$. In addition we have studied the magnetic exponent δ defined through

$$M=H^{1/\delta}g\left[\frac{M^{1/\beta}}{(J-J_c)}\right] .$$

If we run at $J=J_c$ then δ can be extracted from

$$M\sim H^{1/\delta} .$$

II. RESULTS

A. Finite-size scaling and critical indices

We have run on lattices with sizes $N=200$ up to a maximum of $N=3000$ sites, accumulating up to 3×10^7 vector sweeps (a vector sweep in this context attempts to update 20 independent lattice sites and 20 links). Errors are estimated by the usual binning procedure where we demand a plateau in the 20–40 bin region and the susceptibility to agree with its binned average within one standard deviation. As we have argued, ratios of exponents can be extracted from the asymptotic N dependence of observables at the critical coupling J_c. We illustrate this in Fig. 1 (Table I) with a plot of $\ln\chi$ versus $\ln N$ at $J=J_c$. It is clear that the scaling regime only sets in at $N=1000$, and a fit to the last four data points gives us the estimate

$$\frac{\gamma}{\nu d}=0.6(1), \quad \chi^2=0.17 .$$

This is in good agreement with the exact result $\gamma/\nu d=2/3$ and essentially excludes the fixed-lattice number $\gamma/\nu d=7/8$ at three standard deviations. The exponent β describing the critical behavior of the magnetization is, in principle, more difficult to extract, the singular terms vanishing as $N\to\infty$:

$$M\sim N^{-\beta/\nu d} .$$

Nevertheless our log-log plot of M against N (Fig. 2) admits a reasonable linear fit on the six points and gives

$$\frac{\beta}{\nu d}=0.16(1), \quad \chi^2=0.33 .$$

While this number precisely coincides with the exact result for a dynamical lattice $\gamma/\nu d=1/6$, fitting on subsets of the data points yield numbers differing by several standard deviations. This is caused, at least in part, by the onset of critical slowing down on the larger lattices. Therefore the effective error is probably larger than that

TABLE I. χ and M are listed as a function of N for $J=J_c$. The number of Monte Carlo sweeps used in the calculations is also given.

N	M	χ	Sweeps
200	0.69(1)	14.2(8)	1×10^6
500	0.59(1)	33(2)	6×10^6
1000	0.52(2)	68(4)	1.6×10^7
1500	0.49(2)	94(5)	1.6×10^7
2000	0.49(2)	108(8)	2.4×10^7
3000	0.47(2)	134(13)	6×10^7

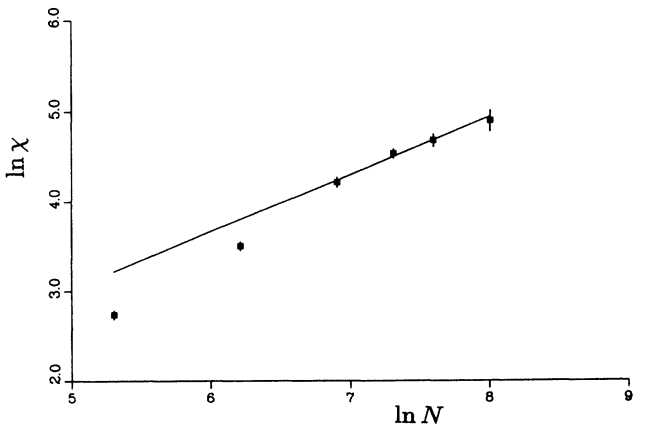

FIG. 1. $\ln\chi$ vs $\ln N$ ($J=J_c$), $N=200$, $N=500$, $N=1000$, $N=1500$, $N=2000$, $N=3000$.

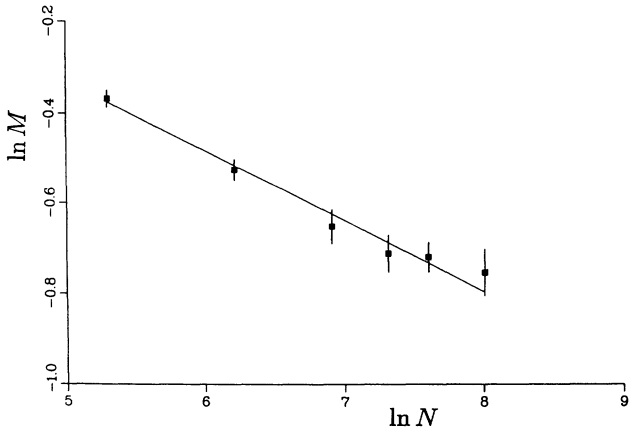

FIG. 2. ln$M$ vs ln$N$ ($J=J_c$), same lattice sizes as above.

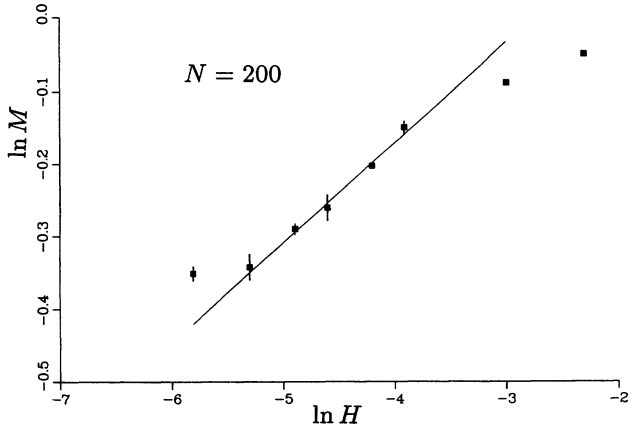

FIG. 3. ln$M$ vs ln$H$ for $N=200$ at $J=J_c$.

quoted above. However, it is certainly very difficult to come up with a fit which is close to the fixed (regular) lattice result of $\beta/\nu d=1/16$. Thus our data, at the very least, exclude such a result and favor the dynamical exponent. Both of these two results are in agreement with an earlier study [9] on triangulated lattices.

To measure the exponent δ we ran on three lattice sizes $N=200$, $N=500$, and $N=1000$ with $J=J_c$ and the addition of a small magnetic field H (Table II). Figure 3 shows a plot of ln$M$ against ln$H$ for $N=200$. At large magnetic field the system is moved out of the critical region and the magnetization saturates. Conversely if the field H is too small finite-size effects dominate and again the magnetization approaches a plateau. Thus the scaling region corresponds to intermediate fields where ln$M$ should have a linear dependence on ln$H$. We see such a window for $0.0075<H<0.015$. A fit gives us an estimate $1/\delta=0.14(2)$, with a $\chi^2=0.5$. In principle, this scaling window should broaden on larger lattices and indeed the data for $N=500$ (Fig. 4) illustrate this with the fitting region extending from $H=0.01$ down to $H=0.002$. A linear fit yields $1/\delta=0.16(1)$, with a $\chi^2=1.0$. This trend continues at $N=1000$ where our data show (Fig. 5), very convincingly, a linear regime extending to small magnetic field. A fit here gives us our best estimate for the exponent

$$\frac{1}{\delta}=0.18(2),\quad \chi^2=0.09\ .$$

This is in excellent agreement with the analytic result $1/\delta=1/5$ and the trend with N shows no sign of running to the fixed-lattice result $1/\delta=1/15$.

Our results thus are generally in good agreement with the analytical results for models with dynamical connectivity and specifically rule out the fixed-lattice exponents. This provides some reassurance that the numerical techniques for summing over triangulations are satisfactory. The fact that scaling sets in for $N\sim1000$ is encouraging for the interpretation of results from such models with extrinsic curvature [5,10] and is in stark contrast to the case of pure two-dimensional gravity, where it is claimed [11] that far larger systems are needed to probe the continuum behavior.

TABLE II. M as a function of H at $J=J_c$ for several lattice sizes.

H	M ($N=200$)	M ($N=500$)	M ($N=1000$)
0.1	0.951(1)		
0.05	0.915(3)	0.919(7)	
0.02	0.861(8)	0.861(2)	0.860(2)
0.015	0.816(4)	0.835(3)	0.860(2)
0.01	0.77(1)	0.795(8)	0.807(5)
0.0075	0.748(6)	0.783(7)	0.781(4)
0.006		0.74(1)	0.754(7)
0.005	0.71(1)	0.71(1)	0.73(1)
0.004			0.71(1)
0.003	0.704(7)	0.67(2)	0.67(1)
0.002		0.62(1)	0.615(9)

B. Scaling functions and equation of state

To attempt a self-consistent check on our results we have constructed finite-size scaling plots for both the susceptibility and magnetization. In Fig. 6 we plot $\ln(\chi N^{-\gamma/\nu d})$ against $\ln(x)$ with $x=\epsilon N^{1/\nu d}$ for $N=500$,

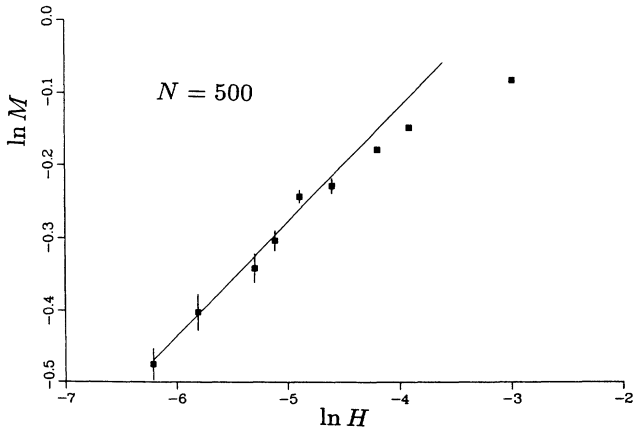

FIG. 4. ln$M$ vs ln$H$ for $N=500$ at $J=J_c$.

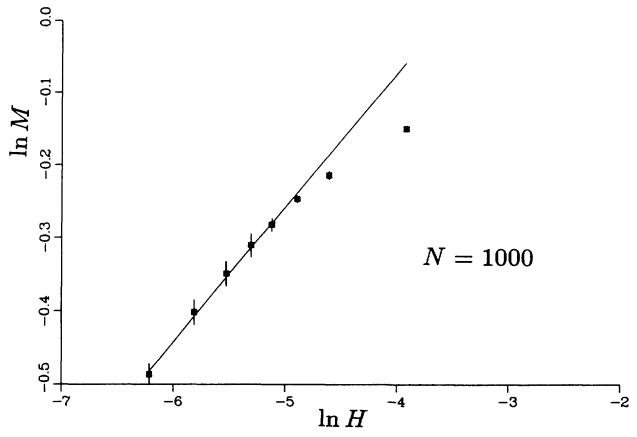

FIG. 5. $\ln M$ vs $\ln H$ for $N=1000$ at $J=J_c$.

$N=1000$, and $N=1500$, assuming the exponents νd, γ take the dynamical lattice values. The data are summarized in Tables III–V. The collapse of the data onto a single curve is indicative of scaling. The slight deviations visible for the $N=500$ data at small x are compatible with our earlier conclusions—that the scaling regime for χ sets in around $N\simeq 1000$. The scaling function $f(x)$ is expected to behave asymptotically as

$$f(x)\sim x^{-\gamma}\ .$$

In principle we can extract an estimate for γ by examining the gradient of the plot at large x. The linear fit shown in the figure yields $\gamma=1.4(1)$ with a $\chi^2=3.0$, which is somewhat different from the analytic prediction $\gamma=2$. However, with the lattice sizes we have considered, we are only about to go to $x\sim 3.0$, which is too small to really probe the limiting behavior. The numerical evidence points to an increase in γ with lattice size, but clearly from this plot alone one cannot distinguish the fixed ($\gamma=\frac{7}{4}$) from dynamical exponent. The equivalent plot for the magnetization $\ln(M^{\beta/\nu d})$ against $\ln(x)$ is shown in Fig. 7. The two branches correspond to

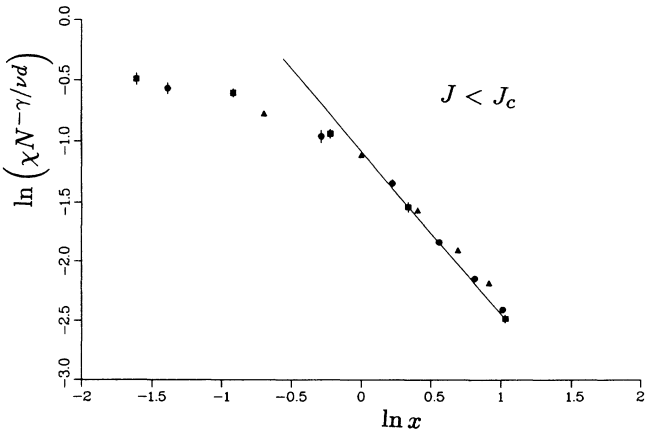

FIG. 6. $\chi N^{\gamma/\nu d}$ vs $x=\epsilon N^{1/\nu d}$. Lattice sizes correspond to $N=500$, 1000, 1500.

TABLE III. Scaling variables $MN^{1/6}$ and $\chi N^{-2/3}$ as a function of β. $N=500$, the external field is zero, and six million sweeps were used per data point.

β	$MN^{1/6}$	$\chi N^{-2/3}$
0.5881	0.455(4)	0.113(2)
0.6177	0.535(3)	0.149(2)
0.6504	0.665(8)	0.208(5)
0.6868	0.86(1)	0.328(6)
0.7275	1.21(2)	0.460(6)
0.733	1.66(4)	0.53(3)
0.8253	2.14(6)	0.42(4)
0.8848	2.50(4)	0.20(5)
0.9535	2.67(1)	0.06(2)
1.0338	2.70(5)	0.06(5)
1.1289	2.792(2)	0.0024(1)

TABLE IV. Scaling variables $MN^{1/6}$ and $\chi N^{-2/3}$ as a function of β. $N=1000$, and the external field is zero. For $\beta<\beta_c$, six million sweeps were used per point. For $\beta>\beta_c$, ten million sweeps were used.

β	$MN^{1/6}$	$\chi N^{-2/3}$
0.6065	0.403(4)	0.090(2)
0.6313	0.464(8)	0.117(3)
0.6581	0.550(8)	0.159(4)
0.6874	0.73(2)	0.260(8)
0.7193	0.96(3)	0.38(2)
0.7544	1.46(5)	0.57(2)
0.7931	1.95(6)	0.57(5)
0.8360	2.50(7)	0.36(7)
0.8838	2.85(3)	0.095(3)
0.9373	2.8(1)	0.17(1)
0.9978	3.067(6)	0.009(2)

TABLE V. Scaling variables $MN^{1/6}$ and $\chi N^{-2/3}$ as a function of β. $N=1500$, and the external field is zero. Twelve million sweeps were used per data point.

β	$MN^{1/6}$	$\chi N^{-2/3}$
0.6213	0.382(7)	0.083(3)
0.6890	0.65(2)	0.214(9)
0.7228	0.94(2)	0.39(1)
0.7472	1.265(6)	0.545(2)
0.7600	1.43(7)	0.61(3)
0.8161	2.39(1)	0.58(9)
0.8639	2.77(8)	0.23(4)

TABLE VI. Equation of state data.

$H/\epsilon^{5/2}$	$M/\epsilon^{1/2}$
1.002	0.95(3)
0.4009	0.69(2)
2.7582	1.60(4)
1.1033	1.23(2)
15.665	3.10(5)
6.2662	2.3(1)
87.9044	4.96(5)
35.1618	4.1(1)
32.0716	3.80(5)
12.8287	3.0(1)

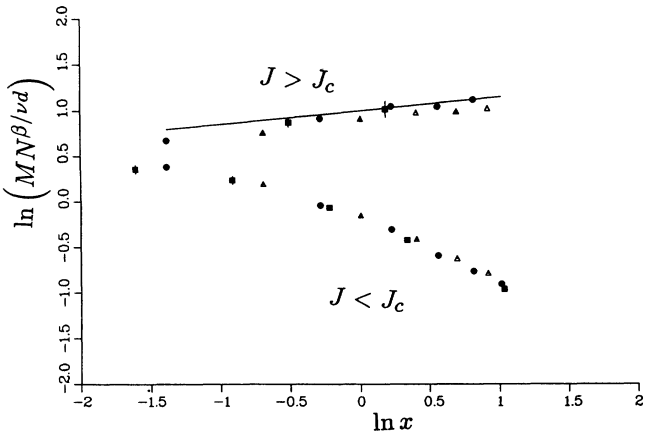

FIG. 7. $MN^{\beta/\nu d}$ against x. Same lattice sizes as above.

the cases $J<J_c$ (lower curve) and $J>J_c$ (upper curve). Again, we have observed earlier, a scaling behavior for the magnetization seems to set in on lattices with only $N=500$ nodes (at least in the high-temperature $J<J_c$ region). A linear fit of the upper branch from $x\sim 1.0$ onwards allows a measurement of β, i.e.,

$$f(x)\sim x^{\beta},\quad x\to\infty\ .$$

The $N=1000$ data yield $\beta=0.25(10)$ with a $\chi^2=2.8$. Furthermore the fits for this exponent yield systematically larger values as N increases. Thus, although we cannot reach large enough x where the fits become stable, the trend in our data would favor the dynamical exponent $\beta=\frac{1}{2}$ rather than its much smaller value on the fixed lattice $\beta=\frac{1}{8}$.

To summarize, we see good evidence for scaling in the finite-size scaling plots and fits to the large-x regime yield further estimates for the exponents β and γ which are compatible with the exact results.

We have also attempted to determine the equation of state

TABLE VII. m vs J for $N=1000$.

J	m
0.50	0.55(2)
0.55	0.42(1)
0.60	0.37(1)
0.65	0.271(4)
0.675	0.234(3)
0.70	0.195(3)
0.725	0.161(2)
0.80	0.128(7)

$$\frac{H}{\epsilon^{\beta\delta}}=\Phi\left[\frac{M}{\epsilon^{\beta}}\right]\ .$$

Using a lattice with $N=1000$ nodes, we determined the magnetization in a scaling region corresponding to small deviations away from the critical point $\epsilon=0.02$–0.12 and small magnetic fields $H=0.002$–0.005. A plot of $H/\epsilon^{\beta\delta}$ against the scaled magnetization M/ϵ^{β} (Fig. 8, Table VI) shows that the data collapse onto a smooth curve which constitutes a nonperturbative measurement of the function Φ.

C. Internal geometry

Finally we have attempted to extract an estimate for the correlation-length exponent ν by a direct measurement of the connected two-point function on the graph. Using a simple algorithm we can construct a map of the intrinsic distance of all points on any particular graph from some reference site. Each lattice link is assinged unit length and the distance between two sites defined as the minimal walk on the graph which connects the two sites. With this information we then form an estimate for the correlator $G(r)$ by averaging over the ensemble of graphs and spin configurations as follows:

$$G(r)=\left\langle \frac{1}{n(r)}\sum_i \sigma_0\sigma_i\delta(d(i)-r)\right\rangle-\langle\sigma_i\rangle^2\ ,$$

$$n(r)=\sum_i \delta(d(i)-r)\ .$$

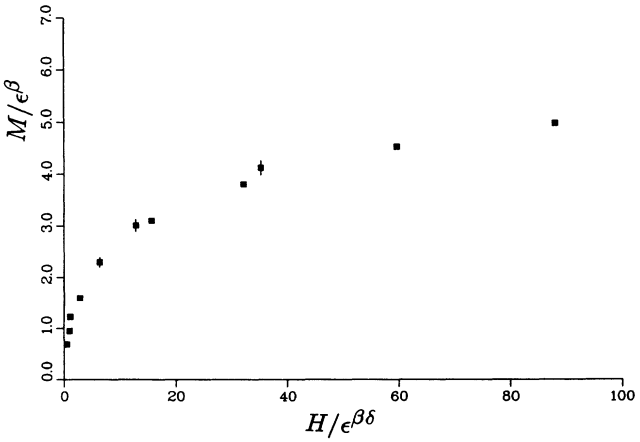

FIG. 8. Equation of state $H/\epsilon^{\beta\delta}$ vs M/ϵ^{β}, $N=1000$.

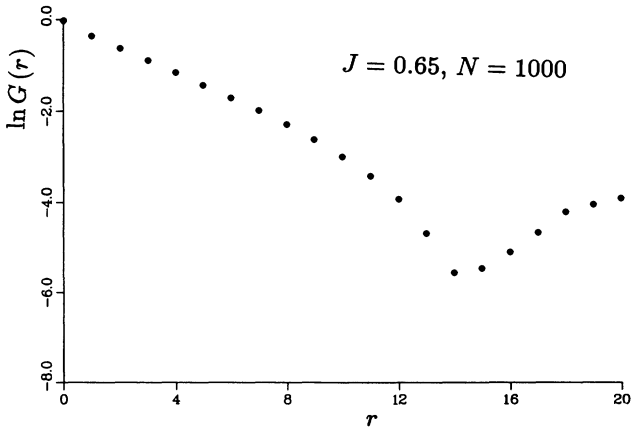

FIG. 9. $\ln G(r)$ vs r at $J=0.65$ with $N=1000$.

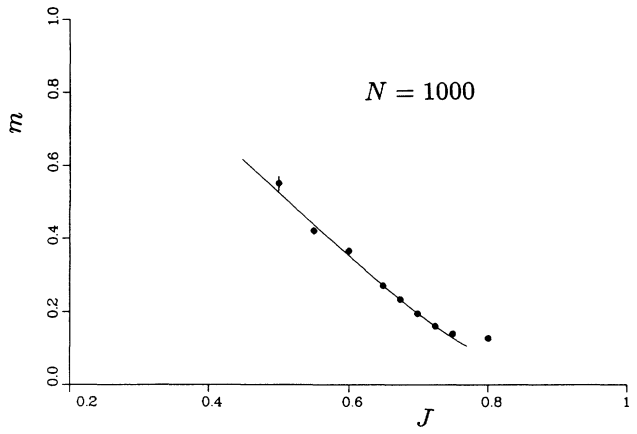

FIG. 10. Mass gap m as a function of coupling J for $N=1000$.

The vector $d(i)$ contains the distance on the graph from site i to the origin i_0. The mass gap is defined from the asymptotic behavior of G:

$$G(r)\sim\exp(-m(J)r), \quad r\to\infty \ .$$

A typical graph of the natural log of the correlation function at $J=0.65$ on a 1000-node lattice is shown in Fig. 9. The linearity of the plot out to lattice distances of order 15 (where the signal is lost in the noise) indicates the dominant contribution of a single state. The fitted masses are shown in Table VII and plotted out as a function of J in Fig. 10. A fit of these data to the form $a+b(J_c-J)^\nu$ yields the estimates $a=0.104(9)$, $b=1.9(2)$, $\nu=1.15(8)$ with a $\chi^2=1.6$. Our data are thus compatible with an exponent of unity, similar to that observed on a fixed lattice. Theory only provides us with the product $\nu d=3$, so our data would favor an internal Hausdorff dimension $d\sim 3$ (notice that this is a purely intrinsic quantity, independent of any "external" Hausdorff dimension associated with embedding the string in some Euclidean space). However it is possible, in principle, to measure d directly by counting the number of lattice sites as a function of distance. Unfortunately we found that d was essentially independent of the Ising coupling J and close to its classical value $d=2$. We interpret this as evidence that the lattices in this study were simply too small to allow for the direct measurement of such nonlocal functions of the geometry as the Hausdorff dimension (see, for example, [11]). Conversely, critical exponents for the Ising sector, being determined by the physics at small scales, may be extracted much more readily.

III. SUMMARY

In this paper we have presented results of finite-size scaling studies of the Ising model on dynamical ϕ^3 graphs. The data show strong evidence for scaling on moderate lattice sizes ($N\sim 1000$), and yield estimates for various critical exponents which are consistent with the results of matrix-model calculations. Our results rule out the fixed-lattice exponents which have been favored by a recent numerical study [7]. We have, in addition, determined the equation of state for the system and analyzed the intrinsic correlations of Ising spins on the graph. The latter leads to an estimate for the correlation exponent ν.

These conclusions are important for the interpretation of other numerical results concerning matter fields (perhaps with $c>1$) coupled to two-dimensional quantum gravity. It would be interesting to extend this analysis to models incorporating further Ising species, in an effort to go continuously through the so-called $c=1$ barrier. It would be highly instructive to find a strong signal of some sort of pathological behavior as the number of Ising species is increased from two to three. Such a signal has been conspicuously lacking in the Gaussian models which have been considered previously; see, e.g., [12].

ACKNOWLEDGMENTS

This work was supported by NSF Grant No. PHY 87-01775 and the numerical calculations were performed using the resources of the Pittsburgh Supercomputer Center and the Ames Research Center. Also, we acknowledge National Science Foundation support through the Materials Research Laboratory at the University of Illinois, Urbana-Champaign, Grant No. NSF-DMR-20538.

[1] J. Ambjorn, B. Durhuus, and J. Frohlich, Nucl. Phys. **B257**, 433 (1985).
[2] F. David, Nucl. Phys. **B257**, 543 (1985).
[3] B. Boulatov, V. Kazakov, I. Kostov, and A. Migdal, Nucl. Phys. **B275**, 641 (1986).
[4] M. Bershadsky and A. Migdal, Phys. Lett. B **174**, 393 (1986).
[5] S. Catterall, J. Kogut, and R. Renken, Nucl. Phys. **B366**, 647 (1991).
[6] D. Boulatov and V. Kazakov, Nucl. Phys. **B186**, 379 (1987); Z. Burda and J. Jurkiewicz, Acta Phys. Pol. B **20**, 949 (1989).
[7] M. Gross and H. Hamber, Report No. UCI-90-33 (unpublished).
[8] E. Domany, K. Mon, G. Chester, and M. Fisher, Phys. Rev. B **12**, 5025 (1975).
[9] J. Jurkiewicz, A. Krzywicki, B. Petersson, and B. Soderberg, Phys. Lett. B **213**, 511 (1988).
[10] S. Catterall, Phys. Lett. B **220**, 207 (1989); R. Renken and J. Kogut, Nucl. Phys. **B354**, 328 (1991).
[11] M. Agishtein, L. Jacobs, A. Migdal, and J. Richardson, MIT Report No. CTP 1840, 1990 (unpublished).
[12] J. Jurkiewicz, A. Krzywicki, and B. Petersson, Nucl. Phys. **B177**, 89 (1986).